Back-action evasion and squeezing of a mechanical resonator using a cavity detector

2008 New J. Phys. 10 095010

(http://iopscience.iop.org/1367-2630/10/9/095010)

New Journal of Physics
The open-access journal for physics

Back-action evasion and squeezing of a mechanical resonator using a cavity detector

A A Clerk[1,4], F Marquardt[2] and K Jacobs[3]

[1] Department of Physics, McGill University, Montréal, Québec, H3A 2T8, Canada
[2] Department of Physics, Arnold-Sommerfeld-Center for Theoretical Physics and Center for NanoScience, Ludwig-Maximilians-Universität München, Theresienstrasse 37, 80333 Munich, Germany
[3] Department of Physics, University of Massachussets at Boston, Boston, MA 02125, USA
E-mail: aashish.clerk@mcgill.ca, florian.marquardt@physik.uni-muenchen.de and kjacobs@cs.umb.edu

New Journal of Physics **10** (2008) 095010 (20pp)
Received 14 April 2008
Published 30 September 2008
Online at http://www.njp.org/
doi:10.1088/1367-2630/10/9/095010

Abstract. We study the quantum measurement of a cantilever using a parametrically coupled electromagnetic cavity which is driven at the two sidebands corresponding to the mechanical motion. This scheme, originally due to Braginsky *et al* (Braginsky V, Vorontsov Y I and Thorne K P 1980 *Science* **209** 547), allows a back-action free measurement of one quadrature of the cantilever's motion, and hence the possibility of generating a squeezed state. We present a complete quantum theory of this system, and derive simple conditions on when the quantum limit on the added noise can be surpassed. We also study the conditional dynamics of the measurement, and discuss how such a scheme (when coupled with feedback) can be used to generate and detect squeezed states of the oscillator. Our results are relevant to experiments in optomechanics, and to experiments in quantum electromechanics employing stripline resonators coupled to mechanical resonators.

[4] Author to whom any correspondence should be addressed.

Contents

1. Introduction

Considerable effort has been devoted recently to attempts at seeing quantum effects in micron to nanometre scale mechanical systems. Experiments coupling such oscillators to mesoscopic electronic position detectors have seen evidence of quantum back-action and back-action cooling [1], and have demonstrated continuous position detection at a level near the fundamental limit placed by quantum back-action [2]–[4]. Complementary to this work, experiments using optomechanical systems (e.g. a cantilever coupled to a optical cavity) have been able to cool micromechanical resonators by several orders of magnitude, using either passive [5]–[8] or active (i.e. feedback-based) approaches [9].

Despite these recent successes, seeing truly quantum behaviour in a mechanical resonator remains a difficult challenge. If one is only doing linear position detection, the quantum behaviour of an oscillator is almost perfectly masked. Nonlinear detector–oscillator couplings allow one to probe quantum behaviour such as energy quantization [10]–[14]; however, generating such couplings is generally not an easy task. Quantum behaviour could also be revealed by coupling the resonator to a qubit [15]–[17]; this too is challenging, as it requires relatively large couplings and a highly phase coherent qubit. Here, we consider an alternate route to seeing quantum behaviour in a mechanical oscillator, one that requires no qubit and only a linear coupling to position. As was first suggested by Braginsky *et al* [18, 19], by using an appropriately driven electromagnetic cavity which is parametrically coupled to a cantilever, one can make a measurement of just a single quadrature of the cantilever's motion. As a result, quantum mechanical back-action need not place a limit on the measurement accuracy, as the back-action affects only the unmeasured quadrature. One can then make (in principle) a perfect measurement of one quadrature of the oscillator's motion. This is in itself useful, as it allows for the possibility of ultra-sensitive force detection [20, 21]. Perhaps even more interesting, one expects that such a measurement can result in a quantum squeezed state of the oscillator, where the uncertainty of the measured quadrature drops below its zero-point value.

While the original proposal by Braginsky is quite old, there nonetheless does not exist a fully quantum theory of the noise and back-action of this scheme; moreover, there exists no treatment of the measurement-induced squeezing. In this paper, we remedy this situation, and

present a fully quantum theory of measurement in this system. We calculate the full noise in the homodyned output signal from the cavity (an experimentally measurable quantity), and derive simple but precise conditions that are needed to beat the conventional quantum limit on the added noise of a position detector [19, 20, 22, 23]. Somewhat surprisingly, we show that beating the standard quantum limit (SQL) does not require a mechanical frequency which is much larger than the cavity damping (i.e. one does not need to be deep in the good-cavity limit). Using a conditional measurement approach, we also discuss the conditions required to squeeze the mechanical resonator, and demonstrate how feedback may be used to unambiguously detect this squeezing. Our results are especially timely, given the recent experimental successes in realizing cavity position detectors using both superconducting stripline resonators [24] as well as optical cavities [5]–[8], [25]; our theory is applicable to both these classes of systems. Note that Ruskov *et al* [26] recently analysed a somewhat related scheme involving stroboscopic measurement of an oscillator with a quantum point contact. Unlike that scheme, the system analysed here should be much easier to implement, being directly related to existing experimental setups; our scheme also has the benefit of allowing significant squeezing without the need to generate extremely fast pulses.

The remainder of this paper is organized as follows. In section 2, we give a heuristic description of how one may realize back-action free single-quadrature detection, introduce the Braginsky two-sideband scheme, and give a synopsis of our main findings. We conclude in section 3, and present a brief discussion on possible experimental realizations. Details of the calculations are relegated to the appendix.

2. Model and main results

2.1. Basic idea behind single quadrature detection

Consider a high-Q mechanical oscillator having frequency ω_{M} and annihilation operator $\hat{c}$. We will use X and Y to denote the cosine and sine quadratures of the oscillator's motion. Using Schrödinger operators $\hat{c}$ and $\hat{c}^{\dagger}$, the operators associated with the quadratures are:

$$\hat{X} = \frac{1}{\sqrt{2}}\left(\hat{c}\mathrm{e}^{\mathrm{i}\omega_{\mathrm{M}}t} + \hat{c}^{\dagger}\mathrm{e}^{-\mathrm{i}\omega_{\mathrm{M}}t}\right), \tag{1a}$$

$$\hat{Y} = -\frac{\mathrm{i}}{\sqrt{2}}\left(\hat{c}\mathrm{e}^{\mathrm{i}\omega_{\mathrm{M}}t} - \hat{c}^{\dagger}\mathrm{e}^{-\mathrm{i}\omega_{\mathrm{M}}t}\right). \tag{1b}$$

The Heisenberg-picture position operator $\hat{x}(t)$ is then given by the Heisenberg-picture operators $\hat{X}(t)$ and $\hat{Y}(t)$ as expected:

$$\hat{x}(t) \equiv \sqrt{2}x_{\mathrm{zpt}}\left(\hat{X}(t)\cos\omega_{\mathrm{M}}t + \hat{Y}(t)\sin\omega_{\mathrm{M}}t\right). \tag{2}$$

Here, x_{zpt} denotes the ground state position uncertainty of the mechanical resonator. Note that $\hat{X}$ and $\hat{Y}$ are canonically conjugate:

$$\left[\hat{X}, \hat{Y}\right] = \mathrm{i}. \tag{3}$$

Also note that the definition of the quadrature operators relies on having an external clock in the system which defines the zero of time.

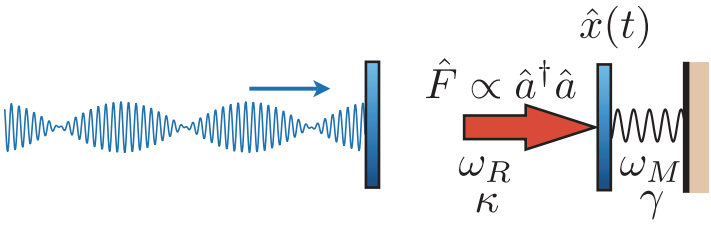

Figure 1. Schematic picture of the setup studied in the text. A cavity is driven by an input beam that is amplitude-modulated at the mechanical frequency $\omega_{\rm M}$ of the movable end-mirror. The radiation pressure force, as well as the cavity and mechanical frequencies and decay rates are indicated.

In general, $\hat{X}(t)$ and $\hat{Y}(t)$ will vary slowly in time (in comparison to $\omega_{\rm M}$) due to the external forces acting on the oscillator. Our goal will be to make a weak, continuous measurement of *only* $\hat{X}(t)$, using the usual kind of setup where the position of the oscillator is linearly coupled to a detector. We will use a detector–oscillator coupling Hamiltonian of the form:

$$\hat{H}_{\rm int} = -\hbar A \hat{x} \hat{F}, \tag{4}$$

where $\hat{F}$ is some detector operator. It represents the force exerted by the detector on the oscillator; in the cavity-position detector we will consider, $\hat{F}$ will be the number of photons in an electromagnetic cavity. Ideally, if we only measure $\hat{X}$, the back-action of the measurement will only affect the unmeasured quadrature $\hat{Y}$, and will not affect the evolution of $\hat{X}$ at later times. The hope thus exists of being able to make a back-action free measurement, one which is not subject to the usual SQL [20, 22, 23].

As is discussed extensively in [20, 21], single quadrature detection with the interaction Hamiltonian in equation (4) can be accomplished by simply modulating the coupling strength A at the oscillator frequency. Setting $A = A(t) = 2(\tilde{A}/x_{\rm zpt})\cos(\omega_{\rm M} t)$, $\hat{H}_{\rm int}$ becomes:

$$\hat{H}_{\rm int} = -\sqrt{2}\hbar \tilde{A} \hat{F} \left[\hat{X} \left(1 + \cos(2\omega_{\rm M} t)\right) + \hat{Y} \sin(2\omega_{\rm M} t) \right]. \tag{5}$$

In a time-averaged sense, we see the detector is only coupled to the X quadrature; we thus might expect that the (time-averaged) output of the detector will tell us only about X. In principle, this in itself does not imply a lack of back-action: via the coupling to $\hat{Y}$, noise in $\hat{F}$ could affect the dynamics of $\hat{X}$. To prevent this, we need the further requirement that *the detector force has no frequency components near* $\pm 2\omega_{\rm M}$. In this case, the effective back-action force $\hat{F}\sin(2\omega_{\rm M} t)$ will have no Fourier weight in the narrow-bandwidth around zero frequency to which $\hat{X}$ is sensitive, and it will not affect $\hat{X}$. Note that Ruskov *et al* [26] recently considered a linear position detection scheme where the effective coupling constant is harmonically modulated; however, their scheme does not satisfy the second requirement above of having a narrow-band back-action force.

2.2. Model

We now consider a specific and experimentally realizable system which can realize the above ideas; this system was first proposed by Braginsky *et al* [18, 19]. As shown schematically in figure 1, the setup consists of a high-Q mechanical oscillator which is parametrically coupled

with strength A to a driven electromagnetic cavity:

$$\hat{H} = \hbar(\omega_{\mathrm{R}} - A\hat{x})\left[\hat{a}^{\dagger}a - \langle\hat{a}^{\dagger}a\rangle\right] + \hat{H}_{\mathrm{M}} + \hat{H}_{\mathrm{drive}} + \hat{H}_{\kappa} + \hat{H}_{\gamma}, \tag{6}$$

where ω_{R} is the cavity resonance frequency, $\hat{H}_{\mathrm{M}} = \hbar\omega_{\mathrm{M}}\hat{c}^{\dagger}\hat{c}$ is the mechanical oscillator Hamiltonian, $\hat{H}_{\mathrm{drive}}$ describes the cavity drive, $\hat{H}_{\kappa}$ describes the cavity damping and $\hat{H}_{\gamma}$ is the mechanical damping. Note this same system was recently shown (in a similar parameter regime to what we will require) to allow back-action cooling to the ground state [27, 28].

Assuming a one-sided cavity, standard input–output theory [29, 30] yields the Heisenberg equation of motion:

$$\dot{\hat{a}} = \left(-\mathrm{i}\omega_{\mathrm{R}} - \frac{\kappa}{2}\right)\hat{a} - \sqrt{\kappa}\,\hat{b}_{\mathrm{in}}(t), \tag{7}$$

where κ is the cavity damping and $\hat{b}_{\mathrm{in}}$ describes both the drive applied to the cavity as well as the noise (quantum and thermal) entering the vacuum port.

To implement back-action evasion in the cavity system, we will consider the case where $\omega_{\mathrm{R}} \gg \omega_{\mathrm{M}}$, and take the resolved-sideband or 'good cavity' limit, where $\omega_{\mathrm{M}} \gg \kappa$. We will also take an amplitude-modulated cavity drive of the form:

$$\langle\hat{b}_{\mathrm{in}}(t)\rangle \equiv \bar{b}_{\mathrm{in}}(t) = \frac{\bar{b}_{\mathrm{LO}}}{2}\sin(\omega_{\mathrm{M}}t)\mathrm{e}^{-\mathrm{i}\omega_{\mathrm{R}}t}. \tag{8}$$

The same resolved-sideband limit is required to achieve ground state cooling [27, 28]; all that is different from the setup here is the nature of the drive. Here, one drives the cavity equally at both sidebands associated with the oscillator motion, whereas in the cooling case, one only drives the red-detuned sideband.

To proceed, we may write the cavity annihilation operator $\hat{a}$ as the sum of a classical piece $\bar{a}(t)$ and a quantum piece $\hat{d}$:

$$\hat{a}(t) = \bar{a}(t) + \hat{d}(t), \tag{9}$$

$\bar{a}(t)$ is determined solely by the response of the cavity to the (classical) external drive $\bar{b}_{\mathrm{in}}(t)$. In the long-time limit, equation (7) yields:

$$\bar{a}(t) = \bar{a}_{\mathrm{max}}\cos\left(\omega_{\mathrm{M}}t + \delta\right)\mathrm{e}^{-\mathrm{i}\omega_{\mathrm{R}}t} \tag{10}$$

with

$$\bar{a}_{\mathrm{max}} = \bar{b}_{\mathrm{LO}}\sqrt{\frac{\kappa}{4\omega_{\mathrm{M}}^2 + \kappa^2}}, \tag{11a}$$

$$\delta = \arctan\left(\kappa/\omega_{\mathrm{M}}\right). \tag{11b}$$

The phase δ plays no role except to set the definitions of the two quadratures X and Y; thus, without loss of generality, we will set it to zero. We will also be interested in a drive large enough that $\bar{a}_{\mathrm{max}} \gg 1$.

In contrast to $\bar{a}$, $\hat{d}$, the quantum part of the cavity annihilation operator, is influenced by both the mechanical oscillator and quantum noise associated with the cavity dissipation. Making use of the solution for $\bar{a}$ and the conditions $\omega_{\mathrm{R}} \gg \omega_{\mathrm{M}} \gg \kappa$, and keeping only terms which are at least order $\bar{a}$, the term in the total system Hamiltonian coupling the oscillator to the cavity takes

an analogous form to equation (5) with:

$$\tilde{A} = \tfrac{1}{2}\left(A x_{\mathrm{zpt}}\right)\bar{a}_{\max}, \tag{12a}$$

$$\hat{F} = \mathrm{e}^{\mathrm{i}\omega_{\mathrm{R}}t}\hat{d} + \mathrm{e}^{-\mathrm{i}\omega_{\mathrm{R}}t}\hat{d}^{\dagger}. \tag{12b}$$

Thus, the chosen cavity drive gives us the required harmonically modulated coupling constant: in a time-averaged sense, the cavity is only coupled to the X-oscillator quadrature. Further, the second condition outlined in section 2.1 is also satisfied: because $\kappa \ll \omega_{\mathrm{M}}$, $\hat{F}$ has no appreciable noise power at frequencies near $\pm 2\omega_{\mathrm{M}}$. As such, we expect no back-action heating of the $\hat{X}$ quadrature in the resolved-sideband limit $\kappa/\omega_{\mathrm{M}} \to 0$. We will of course consider the effect of a nonzero but small $\kappa/\omega_{\mathrm{M}}$ in what follows.

2.3. Back-action

Working in an interaction picture, one can easily derive Heisenberg equations of motion for the system, and solve these in the Fourier domain (cf equations (A.7*a*) and (A.7*b*)). As expected, one finds that in the ideal good-cavity limit ($\kappa/\omega_{\mathrm{M}} \to 0$), the measured X quadrature is completely unaffected by the coupling to the cavity, whereas the unmeasured Y quadrature experiences an extra back-action force due to the cavity. For finite $\kappa/\omega_{\mathrm{M}}$, there is some small additional back-action heating of the X quadrature. The noise spectral densities of the quadrature fluctuations are given by

$$\begin{aligned} S_X(\omega) &\equiv \tfrac{1}{2}\int_{-\infty}^{\infty} \mathrm{d}t\, \mathrm{e}^{\mathrm{i}\omega t}\left\langle\left\{\hat{X}(t), \hat{X}(0)\right\}\right\rangle \\ &= \frac{\gamma/2}{\omega^2 + (\gamma/2)^2}\left[1 + 2\left(n_{\mathrm{eq}} + n_{\mathrm{bad}}\right)\right], \end{aligned} \tag{13a}$$

$$\begin{aligned} S_Y(\omega) &= \tfrac{1}{2}\int_{-\infty}^{\infty} \mathrm{d}t\, \mathrm{e}^{\mathrm{i}\omega t}\left\langle\left\{\hat{Y}(t), \hat{Y}(0)\right\}\right\rangle \\ &= \frac{\gamma/2}{\omega^2 + (\gamma/2)^2}\left[1 + 2\left(n_{\mathrm{eq}} + n_{\mathrm{BA}} + n_{\mathrm{bad}}\right)\right], \end{aligned} \tag{13b}$$

where

$$n_{\mathrm{eq}} = \left(\exp\left[\frac{\hbar\omega_{\mathrm{M}}}{k_{\mathrm{B}}T}\right] - 1\right)^{-1} \tag{14}$$

is the number of thermal quanta in the oscillator. n_{BA} parameterizes the back-action heating of the Y quadrature as an effective increase in n_{eq}; in the relevant limit $\gamma \ll \kappa$ one has:

$$n_{\mathrm{BA}} = \frac{8\tilde{A}^2}{\kappa\gamma} = \frac{2\left(A x_{\mathrm{zpt}}\right)^2}{\kappa\gamma}\left(\bar{a}_{\max}\right)^2. \tag{15}$$

We have assumed here that there is no thermal noise in the cavity drive: it is shot noise-limited.

Finally, n_{bad} parameterizes the spurious back-action heating of X which occurs when one deviates from the good-cavity limit; to leading order in $\kappa/\omega_{\mathrm{M}}$, it is simply given by:

$$n_{\mathrm{bad}} = \frac{n_{\mathrm{BA}}}{32}\left(\frac{\kappa}{\omega_{\mathrm{M}}}\right)^2. \tag{16}$$

Note that there is no back-action damping of either quadrature (see discussion following equation (A.7*b*)).

2.4. Output spectrum and beating the SQL

We assume that a homodyne measurement is made of the light leaving the cavity. Using the solution to the Heisenberg equations of motion (cf equations (A.7*a*) and (A.7*b*)) and standard input–output theory, one can easily find the noise spectral density of the homodyne current $I(t)$. The information about $\hat{X}(t)$ will be contained in a bandwidth $\sim\gamma \ll \kappa$ around zero frequency. Thus, focusing on frequencies $\omega \ll \kappa$, we have simply:

$$S_I(\omega) = G^2\left[S_X(\omega) + \frac{\kappa}{32\tilde{A}^2}S_0\right]. \tag{17}$$

Here, G is a gain coefficient proportional to the homodyne local oscillator amplitude, and S_0 represents added noise in the measurement coming from both the cavity drive and in the homodyne detection. If both are shot noise limited, we simply have $S_0 = 1$. We can refer this noise back to the oscillator by simply dividing out the factor G^2: the result is the *measured* X-quadrature fluctuations:

$$S_{X,\mathrm{meas}}(\omega) \equiv \frac{S_I(\omega)}{G^2} = S_X(\omega) + \frac{\kappa}{32\tilde{A}^2}S_0. \tag{18}$$

Now, note that in the good-cavity limit the spurious heating of X described by n_{bad} vanishes. Thus, in this limit, the added noise term (second term in equation (18)) can be made arbitrarily small by increasing the intensity of the cavity drive beam (and hence $\tilde{A}$), without any resulting back-action heating of the measured X quadrature. Thus, in the good-cavity limit, there is no back-action imposed limit on how small we can make the added noise of the measurement (referred back to the oscillator). In contrast, for small but nonzero $\kappa/\omega_{\mathrm{M}}$, one needs to worry about the small residual backaction described by n_{bad}; one can still, nonetheless, beat the SQL in this case, as we now show.

To compare against the SQL, consider $S_{X,\mathrm{meas}}(0)$:

$$\begin{aligned} S_{X,\mathrm{meas}}(0) &= \frac{2}{\gamma}\left(1 + 2n_{\mathrm{eq}} + 2n_{\mathrm{bad}}\right) + \frac{\kappa}{32\tilde{A}^2}S_0 \\ &\equiv \frac{2}{\gamma}\left(1 + 2n_{\mathrm{eq}} + 2n_{\mathrm{add}}\right). \end{aligned} \tag{19}$$

In the last line, we have represented both the residual back-action n_{bad} and the added noise of the measurement as an effective increase in the number of oscillator quanta by an amount n_{add}. The SQL (which applies when both quadratures are measured) yields the condition $n_{\mathrm{add}} \geqslant 1/2$ [20, 22, 23]. Here, we find:

$$n_{\mathrm{add}} = n_{\mathrm{bad}} + \frac{\kappa\gamma}{128\tilde{A}^2}S_0 = \frac{n_{\mathrm{BA}}}{32}\left(\frac{\kappa}{\omega_{\mathrm{M}}}\right)^2 + \frac{1}{16n_{\mathrm{BA}}}S_0. \tag{20}$$

Thus, if we are in the ideal good-cavity limit ($\kappa/\omega_{\mathrm{M}} \to 0$) and shot-noise limited, beating the SQL on n_{add} requires a coupling strong enough that $n_{\mathrm{BA}} \geqslant 1/8$: the Y quadrature fluctuations must be heated up by at least an eighth of an oscillator quantum.

In the more general case where $\kappa/\omega_{\mathrm{M}}$ is finite, one cannot increase the coupling indefinitely, as there is back-action on $\hat{X}$. One finds that for an optimized coupling of:

$$\tilde{n}_{\mathrm{BA}} = \frac{\omega_{\mathrm{M}}}{\kappa}\sqrt{2S_0}, \tag{21}$$

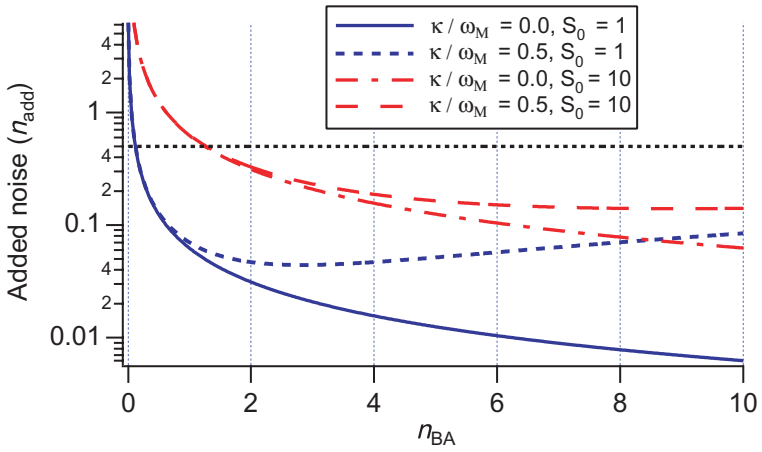

Figure 2. Plot of added noise in the single quadrature measurement (measured as a number of quanta, $n_{\rm add}$, cf equation (20)) versus the strength of the measurement (measured in terms of the back-action heating of the Y quadrature, $n_{\rm BA}$, cf equation (15)). Different curves correspond to different values of $\kappa/\omega_{\rm M}$ and S_0, the noise associated with the homodyne measurement; $S_0 = 1$ corresponds to a shot-noise limited measurement. The SQL of $n_{\rm add} = 0.5$ is shown as a horizontal dashed line.

the minimum added noise at resonance is given by:

$$n_{\rm add}\Big|_{\rm min} = \frac{\kappa}{8\omega_{\rm M}}\sqrt{\frac{S_0}{2}}. \tag{22}$$

Thus, even for moderately small $\kappa/\omega_{\rm M}$, one can make $n_{\rm add}$ smaller than the SQL value (see figure 2). In practice, this fact could be quite valuable, as the large detuning of the cavity drive needed to be in the good-cavity limit can make it hard to get sufficient power in the cavity, and hence achieve a sufficiently strong coupling $n_{\rm BA}$ (cf equation (12*a*)).

2.5. Conditional squeezing

Given that the double-sideband scheme described here can allow for a near perfect measurement of the oscillator X quadrature, one would expect it could lead to a squeezed oscillator state, where the uncertainty in $\hat{X}$ drops below the zero point value of $1/2$. However, equation (13*a*) indicates that in the good-cavity limit, the fluctuations of $\hat{X}$ are *completely* unaffected by the coupling to the cavity detector. To resolve this seeming contradiction, one must consider the *conditional* aspects of the measurement: what is the state of the resonator in a particular run of the experiment? In any given run of the experiment, the oscillator will indeed be squeezed. However, the mean value of $\hat{X}$ will have some nonzero value which is correlated with the noise in the output signal. Once one averages over many realizations of the experiment, this random motion of $\langle\hat{X}\rangle$ appears as extra noise, and masks the squeezing, resulting in the result of equation (13*a*). We make these statements precise in what follows.

A rigorous description of the conditional evolution of the oscillator in the setup considered here can be developed in analogy to [31], which considered ordinary linear position detection using a cavity. For simplicity, we focus on the good-cavity limit, where $\kappa/\omega_{\rm M} \to 0$. We first

define the parameter $\tilde{k}$, a measure of the rate at which the measurement extracts information, as:

$$\tilde{k} = \eta \frac{32\tilde{A}^2}{\kappa} = \eta\,(4\gamma n_{\mathrm{BA}})\,, \tag{23}$$

where n_{BA} represents as before the back-action heating of the Y quadrature, and $\eta = \frac{1}{S_0} \leqslant 1$ represents the efficiency of the homodyne detection ($\eta = 1$ corresponds to being quantum limited). One has $\tilde{k} = 1/\tau_{\mathrm{meas}}$, where τ_{meas} is the minimum time required to resolve a difference in $\langle X\rangle$ equal to the zero point rms value from the output of the detector; as we are interested in weak measurements, we expect $\tilde{k}/\omega_{\mathrm{M}} \ll 1$. Note that $\tilde{k} = 8\eta k$, where k is the usual definition of the strength of the measurement [32]. The scaled homodyne output signal may then be written [32]:

$$I(t) = \sqrt{\tilde{k}}\langle\hat{X}(t)\rangle + \xi(t), \tag{24}$$

where $\xi(t)$ is white Gaussian noise. In a given run of the experiment, $\xi(t)$ will be correlated with the state of the oscillator at times *later* than t.

In exact analogy to [31], a simple description of the conditional oscillator density matrix is possible in the limit where $\kappa \gg \tilde{A}$. In this limit, this density matrix is Gaussian, being fully determined by its means $\bar{X} = \langle\hat{X}\rangle$ and $\bar{Y} = \langle\hat{Y}\rangle$, and its second moments $V_X = \langle\langle\hat{X}^2\rangle\rangle$, $V_Y = \langle\langle\hat{Y}^2\rangle\rangle$ and $C = \langle\langle\{\hat{X}, \hat{Y}\}/2\rangle\rangle$. Note that $\bar{X}$, $\bar{Y}$ represent the observer's best estimates for the oscillator's two quadrature amplitudes, given the measurement output record. In the interaction picture (i.e. rotating frame at the oscillator frequency), the equations for the means (the estimates) are

$$\dot{\bar{X}} = -\frac{\gamma}{2}\bar{X} + \sqrt{\tilde{k}}V_X\xi, \tag{25a}$$

$$\dot{\bar{Y}} = -\frac{\gamma}{2}\bar{Y} + \sqrt{\tilde{k}}C\xi \tag{25b}$$

and for the covariances are

$$\dot{V}_X = -\tilde{k}V_X^2 - \gamma(V_X - \tilde{T}_{\mathrm{eq}}), \tag{25c}$$

$$\dot{V}_Y = -\tilde{k}C^2 + \tilde{k}/(4\eta) - \gamma(V_Y - \tilde{T}_{\mathrm{eq}}), \tag{25d}$$

$$\dot{C} = -\gamma C - \tilde{k}V_X C, \tag{25e}$$

where

$$\tilde{T}_{\mathrm{eq}} = \tfrac{1}{2} + n_{\mathrm{eq}}. \tag{26}$$

We stress that these equations are almost identical to the standard equations for conditional linear position detection [26, 31], with the important exception that terms corresponding to the bare oscillator Hamiltonian are missing. In a sense, the scheme presented here effectively transforms away the oscillator Hamiltonian.

To find the amount of squeezing in a particular run of the experiment, we simply find the stationary variances for the oscillator's Gaussian state. We have

$$V_Y = \tfrac{1}{2} + n_{\mathrm{eq}} + n_{\mathrm{BA}}, \tag{27a}$$

$$V_X = \frac{\sqrt{2\left(1 + 2n_{\mathrm{eq}}\right)(\eta n_{\mathrm{BA}}) + 1/4} - 1/2}{4\,(\eta n_{\mathrm{BA}})}, \tag{27b}$$

$$C = 0. \tag{27c}$$

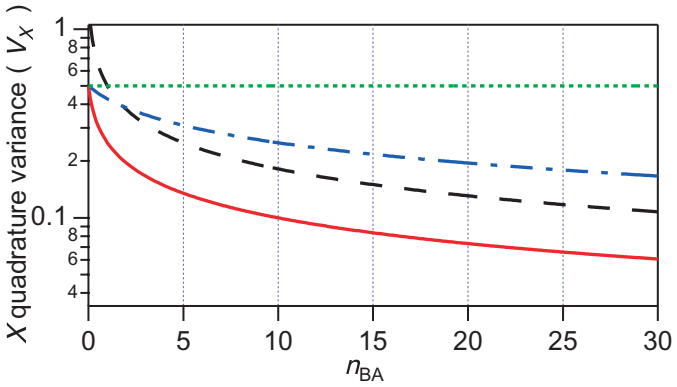

Figure 3. Plot of the *conditional* X-quadrature variance V_X (cf equation (27*b*)) as a function of the measurement strength (parameterized in terms of the back-action heating of the Y quadrature, n_{BA}, cf equation (15)); one clearly sees that the X quadrature can be squeezed. Different curves correspond to different values of the bath temperature (parameterized by n_{eq}, cf equation (14)) and measurement efficiency η. The solid-red curve corresponds to $n_{eq} = 0$ and $\eta = 1$; the dashed black curve to $n_{eq} = 1$ and $\eta = 1$; the dashed-dotted blue curve to $n_{eq} = 0$ and $\eta = 0.1$. The horizontal dashed line corresponds to the ground state value of the variance, $V_X = 0.5$.

Note first that the result for V_Y is in complete agreement with the unconditional result of equation (13*b*): the measurement back-action heats the Y quadrature by an amount corresponding to n_{BA} quanta. In contrast, we find that unlike the unconditional result of equation (13*a*), the measurement causes V_X to decrease below its zero-coupling value: it is a monotonically decreasing function of n_{BA} (see figure 3). This is the expected measurement-induced squeezing. Of particular interest is the minimum coupling strength needed to reduce V_X to its zero-point value:

$$n_{BA} = \frac{n_{eq}}{\eta}. \tag{28}$$

In other words, lowering the X quadrature uncertainty from a thermal value of $(1/2 + n_{eq})$ to the ground state value of $(1/2)$ requires that we *at least* increase the Y-quadrature uncertainty by the same amount. This minimum amount is only achieved for a quantum-limited detector $\eta = 1$.

The equation describing the fluctuations of the mean quadrature amplitudes $\bar{X}$, $\bar{Y}$ can also be easily solved. Assuming that $\bar{X} = \bar{Y} = 0$ at the initial time, one always has $\langle \bar{X}(t) \rangle = \langle \bar{Y}(t) \rangle = 0$, where the average here is over many runs of the experiment. In the stationary state (i.e. once the variances V_X, V_Y and C have attained their stationary values), one finds $\bar{Y}(t) = 0$ with no fluctuations. $\bar{X}(t)$ continues to fluctuate, with an autocorrelation function:

$$\left\langle \bar{X}(t)\bar{X}(0) \right\rangle = \left(\frac{\tilde{k}}{\gamma} \right) V_X^2 \, \mathrm{e}^{-\gamma |t|/2}. \tag{29}$$

Again the average here is over many runs of the experiment.

We may now combine the results of equation (29), and equation (25*c*) to find $V_{X,\mathrm{tot}}$, the total (unconditional) X variance. One finds the simple result (valid in the stationary regime):

$$\begin{aligned} V_{X,\mathrm{tot}} &\equiv V_X + \langle \bar{X}^2 \rangle \\ &= V_X + \frac{\tilde{k}}{\gamma} V_X^2 = \tfrac{1}{2} + n_{\mathrm{eq}}. \end{aligned} \tag{30}$$

This shows that, as expected, averaging the results of the conditional theory over many measurement runs reproduces the result of the unconditional theory (i.e. the fluctuations of the measured X quadrature are completely unaffected by the measurement).

2.6. Feedback for true squeezing

In the previous section, we saw how the state of the resonator, once conditioned on the measurement record, is squeezed. We can use feedback control to turn this conditional squeezing into 'real' squeezing of the resonator, where the full, unconditional oscillator variance $V_{X,\mathrm{tot}}$ (cf equation (30)) drops below the zero-point value. This is accomplished by applying a time-dependent force to the resonator which is proportional to $\bar{X}(t)$, the observer's best estimate of $\langle \hat{X}(t) \rangle$ inferred from the measurement output. Such a force can be used to suppress the fluctuations in the mean value of X, and in the limit of strong feedback, can remove them completely. The only fluctuations that remain are quantified by the conditional variances, which are squeezed. Note that a similar approach was considered in [26].

More precisely, if one makes the measurement at rate $\tilde{k}$ described above (cf equation (23)), and applies the feedback force $F(t) = \alpha\gamma\bar{X}\sin\omega_{\mathrm{M}}t$ in the laboratory frame, the result is in some ways similar to an effective damping of the X quadrature at a rate $\alpha\gamma/2$. Calculating the fluctuations of the X quadrature under this feedback (the details of which are given in the next section), we find that the total unconditioned X-quadrature variance reaches a stationary state:

$$\begin{aligned} V_{X,\mathrm{tot}}^{\mathrm{fb}} &= V_X + \frac{\langle \bar{X}^2 \rangle}{1+\alpha} \\ &= \frac{(n_{\mathrm{eq}} + 1/2) + \alpha V_X}{1+\alpha}. \end{aligned} \tag{31}$$

Here, V_X is the conditioned variance given in equation (27*b*). Note that when $\alpha \to 0$, we again get the result of equation (30): the unconditioned X-quadrature variance is not affected by the measurement. In contrast, in the limit of large α, one has $V_{X,\mathrm{tot}}^{\mathrm{fb}} \to V_X$. Thus, as claimed above, in the limit of strong feedback, the total fluctuations of the X quadrature are reduced to the conditional variance; they may thus be squeezed.

It is also important to ask how this squeezing will manifest itself in the output signal of the measurement. Calculating $S_I^{\mathrm{fb}}(\omega)$, the spectrum of the homodyne current in the presence of feedback, and referring it back to the X quadrature, we find:

$$S_{X,\mathrm{meas}}^{\mathrm{fb}}(\omega) \equiv \frac{S_I^{\mathrm{fb}}(\omega)}{\tilde{k}} = \frac{1}{\tilde{k}} + \frac{(1+\alpha)\gamma V_{X,\mathrm{tot}}^{\mathrm{fb}}}{\omega^2 + \left[(\gamma/2)(1+\alpha)\right]^2}. \tag{32}$$

We see that the output spectrum consists of the white added noise of the measurement $(1/\tilde{k})$ plus a Lorentzian term arising from the oscillator. In the absence of feedback (i.e. $\alpha \to 0$), this term is simply the measurement-independent X-quadrature fluctuation spectrum $S_X(\omega)$; this is in complete agreement with the unconditional theory (cf equation (19)). With the feedback turned

on, the weight of the Lorentzian term is now the total unconditional X-quadrature variance $V^{\rm fb}_{X,\rm tot}$ given in equation (31):

$$\int \frac{{\rm d}\omega}{2\pi}\left(S^{\rm fb}_{X,\rm meas}(\omega)-\frac{1}{\tilde{k}}\right)=V^{\rm fb}_{X,\rm tot}. \tag{33}$$

Thus, using feedback, the output of the measurement can be used to read out the full oscillator X-quadrature variance $V^{\rm fb}_{X,\rm tot}$: one simply measures the integral of the Lorentzian in the output spectrum. In the limit of strong feedback ($\alpha\to\infty$), this variance tends to V_x (the conditional variance), and can exhibit squeezing (cf equation (27*b*)). One thus has a direct way to detect the squeezing generated by the double-sideband back-action evasion scheme.

In practice, there are two potential drawbacks to directly using the output spectrum to detect squeezing. Firstly, in the strong feedback limit $\alpha\to\infty$, the weight of the Lorentzian peak in the spectrum tends to a constant value V_X, but its width diverges as $\alpha\gamma$. For strong feedback, it could thus become very difficult to resolve the Lorentzian term in the output spectrum of equation (32) from the constant background $1/\tilde{k}$. Secondly, one has to worry about accusations that one is not seeing squeezing, but simply noise *squashing* [33]–[35]. This is a phenomenon where feedback reduces fluctuations in the output signal without necessarily reducing the fluctuations of the system being measured. To understand this effect, note that in driving the resonator with a force proportional to $\bar{X}$, we are driving it with a signal that is correlated with the noise in the output signal. Feedback may thus lead to new *correlations* between the fluctuations of X and the output noise. Such correlations could conceivably reduce the oscillator's contribution to the output noise, and are the source of the squashing effect in other systems [35]. In our case, the output spectrum in equation (32) does indeed reflect correlations between the measurement noise and the feedback force. Nonetheless, there is no squashing here, as the weight of the Lorentzian in the output spectrum always coincides with the full variance of the X-quadrature fluctuations. It would still, however, be preferable to have a scheme where one could eliminate the possibility of squashing without any detailed analysis.

A solution to these concerns is to make a second measurement of the mechanical resonator's X quadrature (e.g. by using a second cavity coupled to the resonator). One could then use the corresponding output spectrum to measure the full X-quadrature fluctuations and any potential squeezing. As the output signal from the second measurement, $I_2(t)$, is not part of the feedback loop, its measurement noise is completely uncorrelated with the feedback signal. As a result, there is no unwanted noise correlation, and no possibility of squashing. Surprisingly, the lack of correlations also prevents the apparent bandwidth associated with the oscillator noise from diverging in the strong feedback limit; this point is more fully explained in the appendix.

It is straightforward to calculate the output spectrum of the second measurement. Note that since the second measurement is also a QND measurement of the X quadrature, it does not affect the results for $V^{\rm fb}_{X,\rm tot}$ or $S^{\rm fb}_{X,\rm meas}(\omega)$ derived above. If the rate of the second measurement is $\tilde{\lambda}$, then the spectrum of its output (again, referred back to the oscillator) is

$$S^{\rm fb}_{X,\rm meas,2}(\omega)\equiv\frac{S^{\rm fb}_{I_2}(\omega)}{\tilde{\lambda}}=\frac{1}{\tilde{\lambda}}+\frac{4}{\gamma}\left[\frac{(n_{\rm eq}+1/2)-\mathcal{A}}{(2\omega/\gamma)^2+(1+\alpha)^2}+\frac{\mathcal{A}}{(2\omega/\gamma)^2+\left(1+2\tilde{k}V_X/\gamma\right)^2}\right], \tag{34}$$

where

$$\mathcal{A}=\alpha\frac{(2n_{\rm eq}+1)(1+2\tilde{k}V_X/\gamma+\alpha)-\alpha V_X}{\alpha(2+\alpha)-2(2n_{\rm eq}+1)\tilde{k}/\gamma}. \tag{35}$$

The first term in the spectrum above represents the added noise of the measurement (e.g. shot noise), whereas the terms in square brackets are a direct measure of the oscillator's X-quadrature fluctuations. Unlike the output spectrum of the first, in-loop measurement (cf equation (32)), there is no contribution here from correlations between the measurement noise and feedback force. As a result, the oscillator's contribution to the output spectrum is a sum of two Lorentzians, the integral of which directly yields $V^{\rm fb}_{X,\rm tot}$, the total X-quadrature variance in the presence of feedback

$$\int \frac{{\rm d}\omega}{2\pi}\left(S^{\rm fb}_{X,\rm meas,2}(\omega)-\frac{1}{\tilde{\lambda}}\right)=V^{\rm fb}_{X,\rm tot}. \tag{36}$$

It thus follows from equation (31) that in the strong feedback limit ($\alpha\to\infty$), the area under the resonant peaks in the output spectrum directly yields V_X, and hence a direct measure of squeezing. The same was of course true for the spectrum of I_1 (the in-loop output signal) given in equation (32). However, unlike that spectrum, the bandwidth associated with the oscillator noise here does not become infinite as $\alpha\to\infty$. In this limit, one finds simply

$$\lim_{\alpha\to\infty} S^{\rm fb}_{X,\rm meas,2}(\omega)=\frac{1}{\tilde{\lambda}}+\frac{4}{\gamma_2}\frac{V_x}{(2\omega/\gamma_2)^2+1}, \tag{37}$$

where the effective noise bandwidth γ_2 is given by

$$\gamma_2=\gamma\left(1+2\tilde{k}V_X/\gamma\right)=\gamma\left(1+8n_{\rm BA}V_X\right). \tag{38}$$

Thus, for strong feedback, the squeezing of the oscillator can now be unambiguously detected in the output signal of the second measurement: one obtains a simple Lorentzian resonance whose area is simply V_X. Note that from equation (31), one requires $\alpha\gamma\gg\gamma_2$ in order that the total oscillator variance be reduced to the (possibly squeezed) variance V_X.

3. Experimental prospects and conclusions

We close with a brief discussion of possible experimental realizations of the back-action evasion scheme presented here. One promising class of experiments involves microwave transmission line resonators coupled to nanomechanical resonators. The first experimental realization of such a system was reported by Regal *et al* [24]. These authors were able to achieve $\omega_{\rm M}/\kappa\approx 5$, placing them firmly in the good-cavity limit needed for the double-sideband back-action evasion scheme. Unfortunately, the coupling strength in this first experiment was far too weak to pursue back-action evasion. Assuming one could couple a power of 600 pW to the cavity (as was deemed reasonable by the authors of [24]), the system of [24] yields a coupling-strength parameter $n_{\rm BA}\simeq 10^{-4}$ (cf equation (15)). Recall that beating the SQL requires at least $n_{\rm BA}\geqslant 1/8$. This being said, [24] suggests that it should be possible to increase the coupling strength A by at least a factor of 20. If, in addition, one could use a higher quality mechanical resonator (the current experiment had a mechanical $Q=1.2\times 10^5$) or increase the incident power, one would be in the regime where $n_{\rm BA}$ is large enough to contemplate back-action evasion.

Experiments in optomechanics are also progressing to the point where one can realistically consider implementing the scheme discussed here. The resolved-sideband limit was recently reached by Schliesser *et al* [25] for an optical mode propagating in a microtoroidal cavity that supports mechanical vibrations, with $\omega_{\rm M}/\kappa\approx 20$. Using parameter values provided in [25], and

assuming that a power of 1 μW is coupled to the cavity (as was achieved in the experiment), one finds $n_{\mathrm{BA}} \simeq 0.05$. Thus, the optomechanical setup in [25] is already very close to being able to implement back-action evasion: a modest increase in applied power or oscillator Q factor would allow one to beat the SQL. Note that the chief advantage of the microtoroidal optomechanical system compared to the current version of the microwave cavity system is a much larger intrinsic coupling: the dimensionless ratio $Ax_{\mathrm{zpt}}/\kappa = (\mathrm{d}\omega_{\mathrm{R}}/\mathrm{d}x)x_{\mathrm{zpt}}/\kappa$ is $\sim$1000 times larger in the experiment of [25] versus that in [24].

We now turn to our conclusions. In this paper, we have provided a thorough and fully quantum treatment of back-action evasion using a driven electromagnetic cavity, which is parametrically coupled to a mechanical oscillator. We have considered both the unconditional and conditional aspects of the measurement. In particular, we have derived exactly how strong the coupling must be to beat the SQL, and to achieve a conditionally squeezed state. We have also shown how feedback can be used to generate true squeezing, and how this squeezing can be detected using a second measurement.

Acknowledgments

We thank S Girvin and K Schwab for useful conversations. AC acknowledges the support of NSERC, the Canadian Institute for Advanced Research, and the Alfred P Sloan Foundation. FM acknowledges support by NIM, SFB 631, and the Emmy-Noether program of the DFG.

Appendix. Details of calculations

A.1. Spectrum of the detector output

A.1.1. Equations of motion. The Heisenberg equations of motion (in the rotating frame) follow directly from H_0 and the dissipative terms in the total Hamiltonian:

$$\begin{aligned}\dot{\hat{d}} &= -\frac{\kappa}{2}\hat{d} - \sqrt{\kappa}\hat{\xi}(t)\mathrm{e}^{\mathrm{i}\omega_{\mathrm{R}}t} - \mathrm{i}\tilde{A}\left[\hat{c}\left(1+\mathrm{e}^{-2\mathrm{i}\omega_{\mathrm{M}}t}\right)+\mathrm{h.c.}\right] \\ &= -\frac{\kappa}{2}\hat{d} - \sqrt{\kappa}\hat{\xi}(t)\mathrm{e}^{\mathrm{i}\omega_{\mathrm{R}}t} - \mathrm{i}\sqrt{2}\tilde{A}\left[\hat{X}\left(1+\cos(2\omega_{\mathrm{M}}t)\right)+\hat{Y}\sin(2\omega_{\mathrm{M}}t)\right],\end{aligned} \tag{A.1a}$$

$$\dot{\hat{c}} = -\frac{\gamma}{2}\hat{c} - \sqrt{\gamma}\hat{\eta}(t)\mathrm{e}^{\mathrm{i}\omega_{\mathrm{M}}t} - \mathrm{i}\tilde{A}\left(1+\mathrm{e}^{2\mathrm{i}\omega_{\mathrm{M}}t}\right)\left(\hat{d}+\hat{d}^{\dagger}\right). \tag{A.1b}$$

Here, $\hat{\xi}$ describes noise in the cavity input operator $\hat{b}_{\mathrm{in}}$. In the limit where there is only quantum noise (i.e. shot noise) in the cavity drive, we have

$$\langle\hat{\xi}^{\dagger}(t)\cdot\hat{\xi}(t')\rangle = 0, \tag{A.2a}$$

$$\langle\hat{\xi}(t)\cdot\hat{\xi}^{\dagger}(t')\rangle = \delta(t-t'). \tag{A.2b}$$

In contrast, $\hat{\eta}$ describes equilibrium noise due to the intrinsic damping of the mechanical oscillator. One has

$$\langle\hat{\eta}^{\dagger}(t)\cdot\hat{\eta}(t')\rangle = n_{\mathrm{eq}}\delta(t-t'), \tag{A.3a}$$

$$\langle\hat{\eta}(t)\cdot\hat{\eta}^{\dagger}(t')\rangle = \left(n_{\mathrm{eq}}+1\right)\delta(t-t'), \tag{A.3b}$$

where n_{eq} is a Bose–Einstein occupation factor evaluated at energy $\hbar\omega_{\mathrm{M}}$ and temperature T_{bath}.

The equations of motion are easily solved by first writing them in terms of the quadrature operators $\hat{X}$ and $\hat{Y}$, and then Fourier transforming. To present these solutions, we first introduce the cavity and mechanical oscillator susceptibilities as

$$\chi_{\rm R}(\omega) = \frac{1}{-{\rm i}\omega + \kappa/2}, \tag{A.4a}$$

$$\chi_{\rm M}(\omega) = \frac{1}{-{\rm i}\omega + \gamma/2} \tag{A.4b}$$

and define the back-action force $\hat{f}_{\rm BA}$ via

$$\hat{f}_{\rm BA}(\omega) = -\tilde{A}\sqrt{2\kappa}\,\chi_{\rm R}(\omega)\left(\hat{\xi}(\omega+\omega_{\rm R}) + \hat{\xi}(\omega-\omega_{\rm R})\right). \tag{A.5}$$

Note that while $\hat{\xi}$ describes white noise, the cavity susceptibility $\chi_{\rm R}(\omega)$ ensures that $\hat{f}_{\rm BA}(\omega)$ is only significant around a narrow bandwidth centered about zero frequency. Note also that we define Fourier transformed operators via

$$\hat{A}(\omega) \equiv \int_{-\infty}^{\infty} {\rm d}t\, \hat{A}(t) {\rm e}^{{\rm i}\omega t}, \tag{A.6a}$$

$$\hat{A}^{\dagger}(\omega) \equiv \int_{-\infty}^{\infty} {\rm d}t \left[\hat{A}(t)\right]^{\dagger} {\rm e}^{{\rm i}\omega t}. \tag{A.6b}$$

As such, one has $\left[\hat{A}(\omega)\right]^{\dagger} = \hat{A}^{\dagger}(-\omega)$.

The solutions of the Fourier-transformed quadrature operators then read

$$\hat{X}(\omega) = \chi_{\rm M}(\omega)\left[-\sqrt{\frac{\gamma}{2}}\left(\hat{\eta}(\omega+\omega_{\rm M}) + \hat{\eta}^{\dagger}(\omega-\omega_{\rm M})\right) + \frac{\hat{f}_{\rm BA}(\omega+2\omega_{\rm M}) - \hat{f}_{\rm BA}(\omega-2\omega_{\rm M})}{2{\rm i}}\right], \tag{A.7a}$$

$$\hat{Y}(\omega) = \chi_{\rm M}(\omega)\left[{\rm i}\sqrt{\frac{\gamma}{2}}\left(\hat{\eta}(\omega+\omega_{\rm M}) - \hat{\eta}^{\dagger}(\omega-\omega_{\rm M})\right) - \hat{f}_{\rm BA}(\omega) - \frac{\hat{f}_{\rm BA}(\omega+2\omega_{\rm M}) + \hat{f}_{\rm BA}(\omega-2\omega_{\rm M})}{2}\right]. \tag{A.7b}$$

Note from equations (A.7*a*) and (A.7*b*) that there is no back-action damping of either quadrature, even when one deviates from the good-cavity limit by having $\kappa/\omega_{\rm M} > 0$. This is easy to understand on a purely classical level. Note first that it is only the cosine quadrature (i.e. $\hat{d} + \hat{d}^{\dagger}$) of the cavity which couples to the mechanical resonator. As the cavity is itself a harmonic oscillator, this means that only the cavity sine quadrature (i.e. $\hat{d} - \hat{d}^{\dagger}$) will be affected by the resonator motion. As the cavity cosine quadrature provides the back-action force on the resonator (cf equation (12*b*)), it thus follows that the back-action force is *completely* independent of both quadratures of the mechanical resonator's motion. There is thus no back-action damping, as such damping requires a back-action force which responds (with some time-lag) to the motion of the oscillator.

Equations (13*a*) and (13*b*) for the noise spectra of $\hat{X}$ and $\hat{Y}$ at frequencies $\omega \ll \kappa$ now follow directly from equations (A.7*a*) and (A.7*b*), whereas equations (A.2*a*) and (A.3*a*) determine the noises $\hat{\xi}$ and $\hat{\eta}$.

A.1.2. Output spectrum and beating the SQL. Standard input–output theory [29, 30] yields the following relation between $\hat{b}_{\rm out}$, the field leaving the cavity, and $\hat{b}_{\rm in}$, the field entering the cavity:

$$\hat{b}_{\rm out}(t) = \hat{b}_{\rm in}(t) + \sqrt{\kappa}\hat{a}(t). \tag{A.8}$$

In our case of a one-sided cavity, this relation becomes in the lab (i.e. non-rotating) frame:

$$\hat{b}_{\rm out}(\omega) = \bar{b}_{\rm out}(\omega) + \left[\frac{-{\rm i}(\omega-\omega_{\rm R})-\kappa/2}{-{\rm i}(\omega-\omega_{\rm R})+\kappa/2}\right]\hat{\xi}(\omega) - {\rm i}\tilde{A}\sqrt{2\kappa}\,\chi_{\rm R}(\omega-\omega_{\rm R})\cdot\hat{X}(\omega-\omega_{\rm R}). \tag{A.9}$$

The first term on the rhs simply represents the output field from the cavity in the absence of the mechanical oscillator and any fluctuations. It will yield sharp peaks at the two sidebands associated with the drive, $\omega = \omega_{\rm R} \pm \omega_{\rm M}$. The second term on the rhs of equation (A.9) represents the reflected noise of the incident cavity drive. This noise will play the role of the 'intrinsic output noise' or 'measurement imprecision' of this detector.

Finally, the last term on the rhs of equation (A.9) is the amplified signal: it is simply the amplified quadrature X of the oscillator. We see that the dynamics of $\hat{X}$ will result in a signal of bandwidth $\sim\gamma$ centered at the cavity resonance frequency. This can be detected by making a homodyne measurement of the signal leaving the cavity. Using a local-oscillator amplitude $b_{\rm LO}(t) = {\rm i}B{\rm e}^{-{\rm i}\omega_{\rm R}t}$ with B real, and defining the homodyne current as:

$$\hat{I}(t) = \left(b^*_{\rm LO}(t) + \hat{b}^\dagger_{\rm out}(t)\right)\left(b_{\rm LO}(t) + \hat{b}_{\rm out}(t)\right), \tag{A.10}$$

one finds that the fluctuating part of I is given in frequency-space by

$$\hat{I}(\omega) = -B\left[2\sqrt{2}\tilde{A}\sqrt{\kappa}\,\chi_{\rm R}(\omega)\hat{X}(\omega) + {\rm i}\frac{{\rm i}\omega+\kappa/2}{{\rm i}\omega-\kappa/2}\left(\hat{\xi}(\omega_{\rm R}+\omega) - \hat{\xi}^\dagger(-\omega_{\rm R}+\omega)\right)\right]. \tag{A.11}$$

The signal associated with the oscillator will be in a bandwidth $\sim\gamma \ll \kappa$: for these frequencies, the above expression simplifies to

$$\hat{I}(\omega) = -B\left[\frac{4\tilde{A}}{\sqrt{\kappa/2}}\hat{X}(\omega) + -{\rm i}\left(\hat{\xi}(\omega_{\rm R}+\omega) - \hat{\xi}^\dagger(-\omega_{\rm R}+\omega)\right)\right]. \tag{A.12}$$

Using this equation along with equations (A.7*a*), (A.2*a*) and (A.3*a*), it is straightforward to obtain the result for the homodyne spectrum $S_I(\omega)$ given in equation (17).

A.2. Conditional evolution

To derive the stochastic master equation (SME) describing the conditional evolution of the resonator under the double sideband measurement scheme, (that is, the evolution given the continuous stream of information obtained by the observer), one uses a procedure that is essentially identical to that given in [31]. Once we have moved into the interaction picture (in which the quadratures are QND observables), the displacement picture [36] (that is, separated $\hat{a}$ into $\bar{a}$ and $\hat{d}$ as per equation (9)), and made the rotating-wave approximation, the Hamiltonian for the combined cavity and resonator system is

$$H = -\sqrt{2}\tilde{A}(\hat{d}+\hat{d}^\dagger)X. \tag{A.13}$$

We now perform homodyne detection of output from the (one-sided) cavity, and as a result the evolution of the system is given by the quantum optical SME [36, 37]

$${\rm d}\sigma = -\frac{\rm i}{\hbar}[H,\sigma]\,{\rm d}t + \kappa\mathcal{D}\left[\hat{d}\right]\sigma\,{\rm d}t + \sqrt{\eta\kappa}\,\mathcal{H}\left[-{\rm i}\hat{d}\right]\sigma\,{\rm d}W, \tag{A.14}$$

where σ is the joint density matrix of the two systems as before, η is the detection efficiency, and κ is the cavity decay rate. The superoperators $\mathcal{D}$ and $\mathcal{H}$ are given by

$$2\mathcal{D}[\hat{c}]\sigma = 2\hat{c}\sigma_c\hat{c}^\dagger - \hat{c}^\dagger\hat{c}\sigma - \sigma\hat{c}^\dagger\hat{c}, \tag{A.15}$$

$$\mathcal{H}[\hat{c}]\sigma = \hat{c}\sigma + \sigma\hat{c}^\dagger - \mathrm{Tr}[\hat{c}\sigma + \sigma\hat{c}^\dagger]\sigma, \tag{A.16}$$

for an arbitrary operator $\hat{c}$.

We now wish to obtain an equation for the evolution of the resonator alone. This is possible so long as the cavity decay rate is fast compared to the timescale of the cavity–resonator interaction. That is,

$$\frac{\tilde{A}\sqrt{\langle X^2\rangle}}{\kappa} \sim \frac{\gamma}{\kappa} \equiv \epsilon \ll 1. \tag{A.17}$$

This means that the light ouput from the cavity spends sufficiently little time in the cavity that it continually provides up-to-the-minute information about the oscillator. With this large damping rate, the fluctuations of the light in the cavity about the average value $\bar{a}$ are small, and we can thus expand the cavity state described by the operator $\hat{d}$ about the vacuum

$$\sigma = \rho_{00}|0\rangle\langle 0| + (\rho_{10}|1\rangle\langle 0| + \mathrm{h.c.}) + \rho_{11}^{a}|1\rangle\langle 1| + (\rho_{20}|2\rangle\langle 0| + \mathrm{h.c.}) + O(\epsilon^3). \tag{A.18}$$

The density matrix for the resonator is then given by

$$\rho = \mathrm{Tr}_c[\sigma] = \rho_{00} + \rho_{11} + O(\epsilon^3), \tag{A.19}$$

where Tr_c denotes the trace over the cavity mode. From the master equation (equation (A.14)) we then derive the equations of motion for the ρ_{ij}. Adiabatic elimination of the off-diagonal elements ρ_{01} and ρ_{02} (described in detail in [31]) allows us to write a closed set of equations for the diagonal elements ρ_{00} and ρ_{11}. The result is a SME for $\rho = \rho 00 + \rho 11$, which is

$$\mathrm{d}\rho = k[X,[X,\rho]]\,\mathrm{d}t + \sqrt{2\eta k}\mathcal{H}[X]\rho\,\mathrm{d}W, \tag{A.20}$$

where the measurement strength $k = 4\tilde{A}^2/\kappa$. Defining $\tilde{k} = 8\eta k$, and making a Gaussian ansatz for the quantum state, we find equations (25*a*)–(25*e*) for the means and variances of the quadratures X and Y.

A.3. Squeezing via feedback control

There are three formulations that can be used to analyse the behaviour of an observed linear quantum system: the Heisenberg picture (the input–ouput formalism), the Schrödinger picture (the SME) and the equivalent classical formulation, introduced in [31]. We have already used the first two methods in our analysis above. To analyse the effect of feedback we now use the third. The equivalent classical formulation is given by the equations

$$\mathrm{d}x = -\frac{\gamma}{2}x\,\mathrm{d}t + \sqrt{\gamma\tilde{T}_{\mathrm{eq}}}\,\mathrm{d}W_x, \tag{A.21}$$

$$\mathrm{d}y = -\frac{\gamma}{2}y\,\mathrm{d}t + \sqrt{\gamma\tilde{T}_{\mathrm{eq}}}\,\mathrm{d}W_y + \frac{\sqrt{\tilde{k}}}{2}\,\mathrm{d}V_1 + \frac{\sqrt{\tilde{\lambda}}}{2}\mathrm{d}V_2. \tag{A.22}$$

Here, x and y are the classical dynamical variables which represent the true, fluctuating quadrature amplitudes of the oscillator. The noise sources W_i and V_i are, as always, mutually uncorrelated Wiener processes. We have now included two measurements of the x quadrature,

one with strength $\tilde{k}$ and the other with strength $\tilde{\lambda}$, for reasons that will be explained below. The measurement records (i.e. the homodyned output signals) for these measurements are given by

$$\mathrm{d}I_1 = \sqrt{\tilde{k}}x\,\mathrm{d}t + \mathrm{d}U_1, \tag{A.23}$$

$$\mathrm{d}I_2 = \sqrt{\tilde{\lambda}}x\,\mathrm{d}t + \mathrm{d}U_2. \tag{A.24}$$

Once again the U_i are mutually uncorrelated Wiener processes. Of interest are the quantities $\bar{X}_1$ and $\bar{X}_2$, which are (respectively) the two observers' estimates of the X quadrature. Note that these are *not* the same as x above. When $\tilde{\lambda} = 0$, so that there is no second measurement, the equation of motion for $\bar{X}_1$ is naturally that given by equations (25*a*)–(25*e*). With the second measurement, the dynamics of the means and variances for the first observer become

$$\mathrm{d}\bar{X}_1 = -(\gamma/2)\bar{X}\,\mathrm{d}t + \sqrt{\tilde{k}}V_X\,\mathrm{d}\tilde{U}_1, \tag{A.25a}$$

$$\mathrm{d}\bar{Y}_1 = -(\gamma/2)\bar{Y}\,\mathrm{d}t + \sqrt{\tilde{k}}C\,\mathrm{d}\tilde{U}_1, \tag{A.25b}$$

$$\dot{V}_X = -\tilde{k}V_X^2 - \gamma(V_X - \tilde{T}_{\mathrm{eq}}), \tag{A.25c}$$

$$\dot{V}_Y = -\tilde{k}C^2 + 2k + 2\lambda - \gamma(V_Y - \tilde{T}_{\mathrm{eq}}), \tag{A.25d}$$

$$\dot{C} = -\gamma C - \tilde{k}V_X C, \tag{A.25e}$$

where $k = \tilde{k}/(8\eta_1)$ and $\lambda = \tilde{\lambda}/(8\eta_2)$ are the strengths of the respective measurements (under the usual definition of measurement strength [32]), and the η_i are the respective efficiencies of the measurements. We also introduce a fourth set of noises, $\tilde{U}_i$, where $\tilde{U}_1$ appears in the above equations for the first observer, and $\tilde{U}_2$ would appear in the equations for the second observer, although we will not need those here. The $\tilde{U}_i$ are given by [31]

$$\mathrm{d}\tilde{U}_i = \mathrm{d}I_i - \bar{X}_i\,\mathrm{d}t = \sqrt{\tilde{k}}(x - \bar{X}_i)\,\mathrm{d}t + \mathrm{d}U_i. \tag{A.26}$$

While it is not obvious, it turns out that the $\mathrm{d}\tilde{U}_i$ are also mutually uncorrelated, and uncorrelated with all the other noise sources.

Armed with the above equations, we now introduce feedback into the system. We apply a continuous feedback force $F(t) = \alpha\gamma\bar{X}\sin(\omega_{\mathrm{M}}t)$ to the system in the lab frame. Discarding rapidly oscillating terms (making a rotating-wave approximation), this results in the following dynamics for the system

$$\mathrm{d}x = -\left(\frac{\gamma}{2}x + \frac{\alpha\gamma}{2}\bar{X}_1\right)\mathrm{d}t + \sqrt{\gamma\tilde{T}_{\mathrm{eq}}}\,\mathrm{d}W_x, \tag{A.27}$$

$$\mathrm{d}y = -\frac{\gamma}{2}y\,\mathrm{d}t + \sqrt{\gamma\tilde{T}_{\mathrm{eq}}}\,\mathrm{d}W_y + \sqrt{\tilde{k}/4}\,\mathrm{d}V_1 + \sqrt{\tilde{\lambda}/4}\,\mathrm{d}V_2. \tag{A.28}$$

Note that if $\bar{X}_1 = x$, then the feedback simply provides a damping force on the X quadrature with a rate $\alpha\gamma/2$. As we will see, as $\bar{X}_1$ will not in general be precisely equal to x, the dynamics is in fact slightly more complex.

To proceed, we note that applying a known force to the system cannot change the observers' uncertainty regarding the classical coordinates. Thus, the equations of motion for the variances

for both observers are unaffected by the feedback. The equations of motion for the means, however, also pick up exactly the same damping terms. Thus for observer one we have

$$\dot{\bar{X}}_1 = -\frac{(1+\alpha)\gamma}{2}\bar{X}_1 + \sqrt{\tilde{k}}V_X\dot{\tilde{U}}_1, \tag{A.29}$$

$$\dot{\bar{Y}}_1 = -\frac{\gamma}{2}\bar{Y}_1 + \sqrt{\tilde{k}}C\dot{\tilde{U}}_1. \tag{A.30}$$

We now want to calculate the variance of the X quadrature under this feedback protocol, and also the spectrum of the output signal for both observers. Since the X and Y quadratures are not coupled, we need merely solve the two coupled equations

$$\dot{x} = -\frac{\gamma}{2}x - \frac{\alpha\gamma}{2}\bar{X}_1 + \sqrt{\gamma\tilde{T}_{\rm eq}}\dot{W}_x, \tag{A.31}$$

$$\dot{\bar{X}}_1 = -\left(\frac{\gamma}{2} + \frac{\alpha\gamma}{2} + \tilde{k}V_X\right)\bar{X}_1 + \tilde{k}V_X x + \sqrt{\tilde{k}}V_X\dot{U}_1, \tag{A.32}$$

where we have used equation (26) to write the equation for $\bar{X}_1$ in terms of $\dot{U}_1$ rather than $\dot{\tilde{U}}_1$. The unconditional variance of the X quadrature under feedback, which we will denote by $V^{\rm fb}_{X,\rm tot}$, is given by the variance of x. Solving for the steady-state value of $V^{\rm fb}_{X,\rm tot}$ using the usual techniques of Ito calculus, and using the fact that $\tilde{T}_{\rm eq} = V_X + (\tilde{k}/\gamma)V_X^2$ (cf equation (30)), we obtain equation (31). We see that as the feedback strength α tends to infinity, $V^{\rm fb}_X \to V_X$, as claimed above.

To calculate the spectrum of the output signal for the first observer we first transform equations (A.31) and (A.32) to the frequency domain and solve them. The solution is of the form

$$\begin{pmatrix} x(\omega) \\ \bar{X}_1(\omega) \end{pmatrix} = M(\omega)\begin{pmatrix} \sqrt{\gamma\tilde{T}_{\rm eq}}\dot{W}_x(\omega) \\ \sqrt{\tilde{k}}V_X\dot{U}_1(\omega) \end{pmatrix}, \tag{A.33}$$

with

$$\langle \dot{W}_x(\omega)\dot{W}_x(\omega')\rangle = \langle \dot{U}_1(\omega)\dot{U}_1(\omega')\rangle = \delta(\omega+\omega'). \tag{A.34}$$

The output signal for the first measurement is

$$I_1(\omega) = \sqrt{\tilde{k}}x(\omega) + \dot{U}_1(\omega). \tag{A.35}$$

Note crucially that the first and second terms here are indeed correlated, as the feedback-force driving x depends on the noise $\dot{U}_1$. The output spectrum corresponding to I_1 is defined via

$$\langle I_1(\omega)I_1(\omega')\rangle = S_{I_1}(\omega)\delta(\omega+\omega'). \tag{A.36}$$

Using equations (A.33) and (A.34), and referring the resulting spectrum back to the oscillator by dividing by $\tilde{k}$, we obtain equation (A.32).

Similarly, the output of the second measurement is given by

$$I_2(\omega) = \sqrt{\tilde{\lambda}}x(\omega) + \dot{U}_2(\omega). \tag{A.37}$$

Unlike I_1, the two terms in this equation are completely uncorrelated, as the feedback force applied to x is independent of the added noise $\dot{U}_2$. Using this definition and equations (A.33) and (A.34), and making use of equation (30), we find the output spectrum given in equation (34).

References

[1] Naik A, Buu O, LaHaye M D, Armour A D, Clerk A A, Blencowe M P and Schwab K C 2006 *Nature* **443** 193
[2] Knobel R G and Cleland A N 2003 *Nature* **424** 291
[3] LaHaye M D, Buu O, Camarota B and Schwab K C 2004 *Science* **304** 74
[4] Flowers-Jacobs N E, Schmidt D R and Lehnert K W 2007 *Phys. Rev. Lett.* **98** 096804
[5] Höhberger-Metzger C and Karrai K 2004 *Nature* **432** 1002
[6] Gigan S, Böhm H, Paternostro M, Blaser F, Hertzberg J B, Schwab K C, Bauerle D, Aspelmeyer M and Zeilinger A 2006 *Nature* **444** 67–70
[7] Schliesser A, Del'Haye P, Nooshi N, Vahala K J and Kippenberg T J 2006 *Phys. Rev. Lett.* **97** 243905
[8] Thompson J D, Zwickl B M, Jayich A M, Marquardt F, Girvin S M and Harris J G E 2008 *Nature* **452** 06715
[9] Kleckner D and Bouwmeester D 2006 *Nature* **444** 75–8
[10] Santamore D H, Doherty A C and Cross M C 2004 *Phys. Rev.* B **70** 144301
[11] Jacobs K, Lougovski P and Blencowe M P 2007 *Phys. Rev. Lett.* **98** 147201
[12] Martin I and Zurek W H 2007 *Phys. Rev. Lett.* **98** 120401
[13] Buks E, Arbel-Segev E, Zaitsev S, Abdo B and Blencowe M P 2008 *Europhys. Lett.* **81** 10001
[14] Jacobs K, Jordan A N and Irish E K 2008 *Europhys. Lett.* **82** 18003
[15] Armour A D, Blencowe M P and Schwab K C 2002 *Phys. Rev. Lett.* **88** 148301
[16] Wei L F, Liu Y X, Sun C P and Nori F 2006 *Phys. Rev. Lett.* **97** 237201
[17] Clerk A A and Utami D W 2007 *Phys. Rev.* A **75** 042302
[18] Braginsky V B, Vorontsov Y I and Thorne K P 1980 *Science* **209** 547–57
[19] Braginsky V B and Khalili F Y 1992 *Quantum Measurement* (Cambridge: Cambridge University Press)
[20] Caves C M, Thorne K S, Drever R W P, Sandberg V D and Zimmermann M 1980 *Rev. Mod. Phys.* **52** 341–92
[21] Bocko M F and Onofrio R 1996 *Rev. Mod. Phys.* **68** 755–99
[22] Caves C M 1982 *Phys. Rev.* D **26** 1817–39
[23] Clerk A A 2004 *Phys. Rev.* B **70** 245306
[24] Regal C A, Teufel J D and Lehnert K W 2008 *Nat. Phys.* **4** 555
[25] Schliesser A, Rivière R, Anetsberger G, Arcizet O and Kippenberg T J 2008 *Nat. Phys.* **4** 415
[26] Ruskov R, Schwab K and Korotkov A N 2005 *Phys. Rev.* B **71** 235407
[27] Marquardt F, Chen J P, Clerk A A and Girvin S M 2007 *Phys. Rev. Lett.* **99** 093902
[28] Wilson-Rae I, Nooshi N, Zwerger W and Kippenberg T J 2007 *Phys. Rev. Lett.* **99** 093901
[29] Walls D F and Milburn G J 1995 *Quantum Optics* (New York: Springer)
[30] Gardiner C W and Zoller P 2000 *Quantum Noise* (Berlin: Springer)
[31] Doherty A C and Jacobs K 1999 *Phys. Rev.* A **60** 2700
[32] Jacobs K and Steck D A 2006 *Contemp. Phys.* **47** 279
[33] Buchler B C, Gray M B, Shaddock D A, Ralph T C and McClelland D E 1999 *Opt. Lett.* **24** 259
[34] Wiseman H M 1999 *J. Opt. B: Quantum Semiclass. Opt.* **1** 459
[35] Poggio M, Degen C L, Mamin H J and Rugar D 2007 *Phys. Rev. Lett.* **99** 017201
[36] Wiseman H M and Milburn G J 1993 *Phys. Rev.* A **47** 642
[37] Carmichael H 1993 *An Open Systems Approach to Quantum Optics* (Berlin: Springer)